Cubic and Columnar Supramolecular Architectures of Rod–Coil Molecules in the Melt State**

Myongsoo Lee,* Byoung-Ki Cho, Heesub Kim, and Wang-Cheol Zin

Diblock molecules consisting of a rigid rod block and a flexible coil block provide the opportunity to study novel aspects of liquid-crystalline supramolecular structures. In general, classical rodlike molecules are arranged with their long axes parallel to each other to give rise to nematic and/or layered smectic types of supermolecular structures in the melt state. In contrast, diblock molecules consisting of different immiscible coil segments induce columnar or cubic types of supramolecular assemblies in addition to lamellar structures in a selective solvent.[1] Unlike rodlike molecules, coil–coil diblock copolymers also self-assemble into various supramolecular architectures with curved interfaces in the melt state due to conformational freedom associated with a long flexible chain.[2] A combination of these structural principles can provide a novel class of self-assembling materials since this rod–coil diblock system shares certain general characteristics of both lyotropic diblock molecules and thermotropic calamitic molecules.

Rod–coil molecules show lamellar or micellar microphase-separated domains depending on the volume fraction of coil segments in the molecules, although molecular order within the rod blocks in the melt state was not described.[3] In 1996 we published[4, 5] that rod–coil molecules consisting of a molecular rod and a poly(ethylene oxide) coil exhibit a microphase-separated lamellar structure of nanoscale dimensions in the crystalline phase as well as in the melt state; this leads to a smectic supramolecular structure. The binary mixture of these rod–coil molecules and lithium triflate induces micellar mesophases that are dependent on the salt concentrations.[5] This experimental system enabled us to study further their thermotropic phase behavior.

The design of the rod–coil diblock molecules was based on an extended rodlike molecule consisting of two biphenyl units.[4–6] The extended rods of this type can exhibit calamitic mesomorphism; however, unlike amphiphilic diblock macromolecules, rod molecules cannot form cubic or columnar phases with curved interfaces owing to steric reason. To introduce block segregation character, we synthesized rod–coil diblock molecules **1**–**3** consisting of a molecular rod and a poly(propylene oxide) coil (Figure 1). The coil portion is bulkier than poly(ethylene oxide) at the same degree of polymerization and is not able to crystallize because of the side methyl group in the propylene oxide unit. Therefore, these rod–coil diblock molecules can be considered as either small block copolymers or large smectogens.

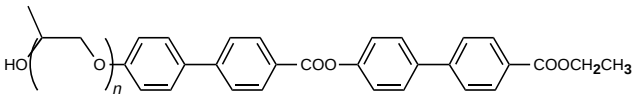

1 n=7 k 62.1 s_C 108.6 s_A 122.8 i

2 n=12 k 38.7 bcc 69.6 i

3 n=15 k 23.0 bcc 41.1 col 46.1 i

Figure 1. Structure and phase behavior of **1**–**3**. The transition temperatures are given in °C; k: crystalline; s_A: smectic A; s_C: smectic C; bcc: bicontinuous cubic; col: hexagonal columnar; i: isotropic phase. The phase-transition temperatures are obtained from the second heating curves of the DSC measurements with a scan rate of 3 °C min^{-1}.

Rod–coil molecules **1**–**3** (see Table 1 for spectroscopic data) containing poly(propylene oxide) groups with various degrees of polymerization n were synthesized by a procedure similar to that previously described.[4, 6] The resulting rod–

Table 1. Spectroscopic data of **1**–**3**.

1: ^{1}H NMR (250 MHz, $CDCl_3$, TMS): $\delta = 8.26$ (d, $J = 8.2$ Hz, 2H; *o* to COOphenyl), 8.13 (d, $J = 8.2$ Hz, 2H; *o* to $COOCH_2$), 7.65–7.72 (m, 6H; *m* to COOphenyl, *m* to biphenylcarboxylate, and *m* to $COOCH_2$), 7.60 (d, $J =$ 8.6 Hz, 2H; *m* to $CH(CH_3)O$), 7.34 (d, $J = 8.4$ Hz, 2H; *o* to biphenylcarboxylate), 7.04 (d, $J = 8.3$ Hz, 2H; *o* to $CH(CH_3)O$), 4.58 (m, 1H; $OCH_2CH(CH_3)$), 4.41 (q, $J = 7.1$ Hz, 2H; CH_2CH_3), 3.18–3.92 (m, 20H; OCH_2CH), 1.35–1.45 (m, 6H; CH_2CH_3 and $CH(CH_3)$Ophenyl), 0.90–1.30 (m, 18H; $OCH_2CH(CH_3)$); ^{13}C NMR (62.5 MHz, $CDCl_3$, TMS): $\delta = 166.4$, 165.0, 158.6, 158.5, 151.1, 146.0, 144.6, 137.7, 132.1, 130.7, 130.1, 129.3, 128.3, 127.3, 126.9, 126.6, 122.2, 116.4, 72.3–76.0, 67.2, 65.5, 61.0, 18.4–16.9, 14.3; elemental analysis calcd for $C_{49}H_{64}O_{12}$: C 69.65, H 7.63; found: C 69.69, H 7.30.

2: ^{1}H NMR (250 MHz, $CDCl_3$, TMS): $\delta = 8.24$ (d, $J = 7.8$ Hz, 2H; *o* to COOphenyl), 8.12 (d, $J = 7.7$ Hz, 2H; *o* to $COOCH_2$), 7.65–7.71 (m, 6H; *m* to COOphenyl, *m* to biphenylcarboxylate, and *m* to $COOCH_2$), 7.59 (d, $J =$ 8.5 Hz, 2H; *m* to $CH(CH_3)O$), 7.34 (d, $J = 8.5$ Hz, 2H; *o* to biphenylcarboxylate), 7.04 (d, $J = 8.6$ Hz, 2H; *o* to $CH(CH_3)O$), 4.58 (m, 1H; $OCH_2CH(CH_3)$), 4.41 (q, $J = 7.1$ Hz, 2H; CH_2CH_3), 3.15–3.91 (m, 35H; OCH_2CH), 1.34–1.45 (m, 6H; CH_2CH_3 and $CH(CH_3)$Ophenyl), 0.90–1.30 (m, 33H; $OCH_2CH(CH_3)$); ^{13}C NMR (62.5 MHz, $CDCl_3$, TMS): $\delta = 166.4$, 165.0, 158.6, 158.5, 151.1, 146.1, 144.7, 137.8, 132.1, 130.7, 130.1, 129.3, 128.4, 127.3, 127.0, 126.6, 122.2, 116.4, 72.9–75.5, 67.2, 65.6, 61.0, 16.9–18.4, 14.3; elemental analysis calcd for $C_{64}H_{94}O_{17}$: C 67.70, H 8.34; found: C 67.72, H 8.48.

3: ^{1}H NMR (250 MHz, $CDCl_3$, TMS): $\delta = 8.25$ (d, $J = 7.8$ Hz, 2H; *o* to COOphenyl), 8.12 (d, $J = 7.7$ Hz, 2H; *o* to $COOCH_2$), 7.65–7.71 (m, 6H; *m* to COOphenyl, *m* to biphenylcarboxylate, and *m* to $COOCH_2$), 7.59 (d, $J =$ 8.5 Hz, 2H; *m* to $CH(CH_3)O$), 7.31 (d, $J = 8.5$ Hz, 2H; *o* to biphenylcarboxylate), 7.04 (d, $J =$ 8.6 Hz, 2H; *o* to $CH(CH_3)O$), 4.58 (m, 1H; $OCH_2CH(CH_3)$), 4.41 (q, $J = 7.1$ Hz, 2H; CH_2CH_3), 3.15–3.92 (m, 44H; OCH_2CH), 1.34–1.45 (m, 6H; CH_2CH_3 and $CH(CH_3)$Ophenyl), 0.85–1.35 (m, 42H; $OCH_2CH(CH_3)$); ^{13}C NMR (62.5 MHz, $CDCl_3$, TMS): $\delta = 166.4$, 165.0, 158.6, 158.5, 151.0, 146.0, 144.6, 137.7, 132.0, 130.7, 130.1, 129.3, 128.3, 127.3, 126.9, 126.6, 122.2, 116.3, 72.6–76.0, 67.1, 65.5, 60.9, 16.9–18.4, 14.3; elemental analysis calcd for $C_{73}H_{112}O_{20}$: C 66.95, H 8.62; found: C 67.24, H 8.71.

[*] Prof. M. Lee, B.-K. Cho
Department of Chemistry
Yonsei University
Shinchon 134, Seoul 120-749 (Korea)
Fax: (+82) 2-364-7050
E-mail: mslee@alchemy.yonsei.ac.kr
H. Kim, Prof. W.-C. Zin
Department of Materials Science and Engineering
Pohang University of Science and Technology (Korea)

[**] This work was supported by the Ministry of Education Republic of Korea (BSRI 96-3422) and the Korea Science and Engineering Foundation (1996)

  1433-7851/98/3705-0638 $ 17.50+.50/0

coil molecules were characterized by differential scanning calorimetry (DSC) and thermal optical polarized microscopy (Figure 1). Upon heating of **1** ($n=7$) the crystalline phase goes into a smectic C phase at 62.1 °C, which in turn undergoes transformation into a smectic A phase.

In contrast, no birefringence between crossed polarizers could be observed upon melting of **2** ($n=12$) at 38.7 °C. The DSC results indicate an additional phase transition at 69.6 °C, which is accompanied by a significant decrease in viscosity; this strongly suggests the existence of a cubic mesophase in the range of 38.7 – 69.6 °C.[7] This is also confirmed by X-ray scattering experiments, which exhibit the same diffraction pattern (except that the lattice constant is smaller) as for the low-temperature mesophase of **3**.

Rod – coil molecule **3** ($n=15$) exhibits a crystalline melting transition into an optical isotropic cubic mesophase followed at higher temperatures by a hexagonal columnar mesophase, which in turn undergoes isotropization at 46.1 °C. Upon cooling the isotropic liquid, a spherulitic growing of texture can first be observed with a final development of pseudo-focal conic domains that are characteristic of a hexagonal columnar mesophase of conventional discotic mesogens.[8] On further cooling the hexagonal columnar phase, isotropic rectangular and rhombic areas with straight edges appear on the pseudo-focal conic domains. These regions then grow until the entire field of view is dark; this behavior is characteristic of the cubic mesophase (Figure 2).[7]

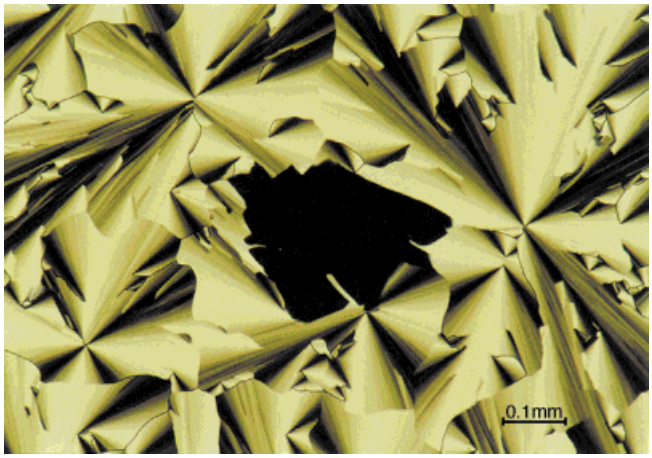

Figure 2. Representative optical polarized micrograph (100 × magnification) of the texture of **3** observed at the transition from the hexagonal columnar phase (pseudo-focal conic domains) to the cubic phase (dark area with straight edges) at 41 °C upon cooling.

To confirm the assignments of the mesophases, both small-angle (SAXS) and wide-angle X-ray scattering (WAXS) experiments were performed with **3** at various temperatures (Figure 3). The X-ray diffraction pattern of **3** in the crystalline state displays three reflections with q spacings of 0.84, 1.64, and 2.44 nm^{-1} in the small-angle region (Figure 3a), whereas two sharp reflections are observed in the wide-angle region. From the analysis of all available data, we can conclude that the crystalline phase of **3** is a lamellar structure with a periodicity of 7.5 nm. Comparison with the calculated length

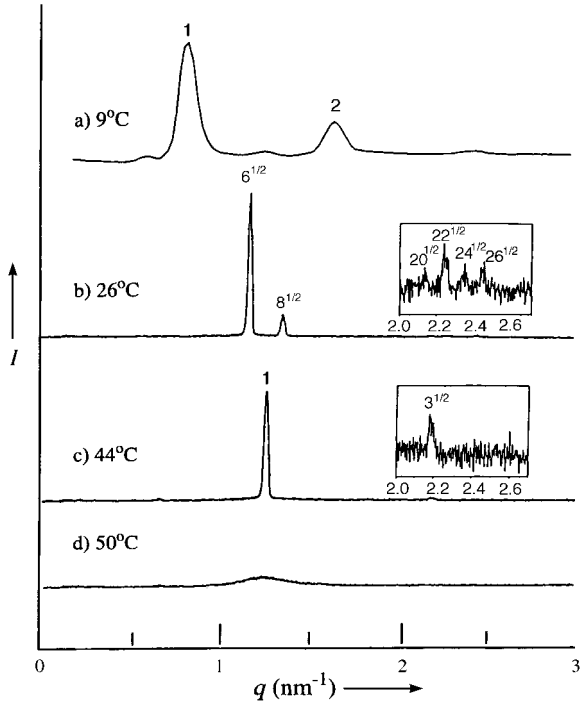

Figure 3. SAXS spectra of **3** obtained at different temperatures plotted against q ($=4\pi\sin\theta/\lambda$). Spectrum (a) was measured with Ni-filtered $Cu_{K\alpha}$ radiation and corrected for slit-length smearing. Spectra (b) through (d) were measured with synchrotron radiation at the 3C2 X-ray beam line ($\lambda=$ 0.1608 nm) at the Pohang Accelerator Laboratory.

of a fully extended molecular unit of 8.6 nm suggests that this periodicity arises from monolayers with packing similar to that in a related rod – coil molecule.[5]

In the liquid-crystalline phase at 26 °C, two strong and four weak reflections are observed at the relative positions $\sqrt{6}$, $\sqrt{8}$, $\sqrt{20}$, $\sqrt{22}$, $\sqrt{24}$, and $\sqrt{26}$ (Figure 3b). The positions of these reflections can be indexed as the (211), (220), (420), (332), (442), and (431) reflections of *Ia*3*d* symmetry.[9] From the observed d spacing of the (211) reflection, the value giving the best fit for the cubic lattice parameter a is 13.2 nm. At a wide angle only a diffuse halo remains as evidence for the melting of the aromatic rods. On the basis of the X-ray diffraction data described above and the thermal behavior, which exhibits an intermediate phase between the lamellar and columnar structures, the cubic phase can be best described as a bicontinuous cubic phase with *Ia*3*d* symmetry.[2, 9]

Upon further heating to 45 °C, **3** displays two sharp reflections with q spacings of 1.25 and 2.14 nm^{-1} whose SAXS pattern obeys the ratio of $1:\sqrt{3}$ (Figure 3c), which is characteristic of the two-dimensional hexagonal structure (hexagonally packed array of cylindrical micelles).[2] In contrast, only a diffuse halo can be observed in the WAXS pattern. These results together with observations from optical microscopy support that the high-temperature mesophase of **3** displays a disordered hexagonal columnar mesophase with a lattice constant of 5.8 nm. In the isotropic phase, **3** shows only broad, diffuse scattering in the small-angle region, which is most probably due to the existence of dynamic density inhomogeniety in the diblock melt.

Such molecular organizations in molecular rods are in striking contrast to what is generally accepted for the

  1433-7851/98/3705-0639 $ 17.50+.50/0

relationship between molecular structure and the mesomorphic phase of thermotropic liquid crystals. The phase behavior in our rod–coil system can be explained by the fact that the main factor governing the geometry of the supramolecular architecture in the liquid-crystalline phase is the anisotropic aggregation of rod segments and the consequent space-filling requirements as well as entropic limitations due to the flexibility of the coil.[10–13] The lamellar structure observed in the crystalline phase for **3** or in the liquid -crystalline phase for **1** is still the most efficient packing of melt chains, which is similar to that of smectogens with low molar mass. With increasing temperature (in the case of **3**) or increasing volume fraction of coil segments, however, space crowding of the coil segments would be larger. Lamellar ordering of rods would confine junctions between rods and coils to a flat interface with a relatively high density of grafting sites, which forces a strong stretching of the coils away from the interface, and the system becomes energetically unfavorable. Consequently, the lamellar structure of the rod–coil molecule will break apart into interwoven networks of branched cylinders to lead to a bicontinuous cubic phase and then discrete cylinders; this gives rise to a hexagonal columnar phase in which coil stretching is reduced.

Although this explanation is qualitatively consistent with theoretical predictions for the phase behavior of rod–coil diblock molecules, that of our system is in contrast to the predicted specific supramolecular structures such as the various "hockey-puck" phases.[11] In this respect, our system provides access to a large variety of experimental and theoretical investigations to understand fully the complete range of supramolecular structures formed by rod–coil diblock molecules. This is essentially an unexplored area of research.

In summary, the rod–coil molecules which can be considered as either small diblock copolymers or large smectogens were observed to organize into bicontinuous cubic and hexagonal columnar mesophases as a function of volume fraction of the coil segments or temperature. This behavior differs significantly from that predicted for this type of molecule.[10–13]

Received: September 2, 1997 [Z 10881 IE]
German version: *Angew. Chem.* **1998**, *110*, 661–663

Keywords: columnar phases · cubic phases · liquid crystals · mesophases · supramolecular chemistry

[1] "Liquid Crystals": H. Stegemeyer, *Top. Phys. Chem.* **1994**, *3*.
[2] M. A. Hillmyer, F. S. Bates, K. Almdal, K. Mortensen, A. J. Ryan, J. P. Fairclough, *Science* **1996**, *271*, 976–978; F. S. Bates, *ibid.* **1991**, *251*, 898–901; S. Foster, A. K. Khandpur, J. Zhao, F. S. Bates, I. W. Hamley, A. J. Ryan, W. Bras, *Macromolecules* **1994**, *27*, 6922–6935.
[3] J. T. Chen, E. L. Thomas, C. K. Ober, G. Mao, *Science* **1996**, *273*, 343–346; J. T. Chen, E. L. Thomas, C. K. Ober, S. S. Hwang, *Macromolecules* **1995**, *28*, 1688–1697; L. H. Ladzilowski, B. O. Carraher, S. I. Stupp, *ibid.* **1997**, *30*, 2110–2119; L. H. Ladzilowski, S. I. Stupp, *ibid.* **1994**, *27*, 7747–7753; S. I. Stupp, V. LeBonheur, K. Walker, L. S. Li, K. E. Huggins, M. Keser, A. Amstutz, *Science* **1997**, *276*, 384–389. We thank a referee for bringing our attention to this work.
[4] M. Lee, N.-K. Oh, *J. Mater. Chem.* **1996**, *6*, 1079–1086.
[5] M. Lee, N.-K. Oh, H.-K. Lee, W.-C. Zin, *Macromolecules* **1996**, *29*, 5567–5573; M. Lee, N.-K. Oh, *Mol. Cryst. Liq. Cryst.* **1996**, *280*, 283–288.
[6] M. Lee, N.-K. Oh, W.-C. Zin, *Chem. Commun.* **1996**, 1787–1788.
[7] D. Demus, L. Richter, *Texture of Liquid Crystals*, Verlag Chemie, Weinheim, **1978**; G. W. Gray, J. W. Goodby, *Smectic Liquid Crystals, Texture and Structures*, Leonard Hill, Glasgow, **1984**.
[8] C. Destrade, P. Foucher, H. Gasparoux, N. H. Tinh, A. M. Levelut, J. Malthete, *Mol. Cryst. Liq. Cryst.* **1984**, *106*, 121–146; C. Destrade, N. H. Tinh, H. Gasparoux, J. Malthete, A. M. Levelut, *ibid.* **1981**, *71*, 111–117.
[9] J. M. Seddon, *Biochemistry* **1990**, *29*, 7997–8002; V. Luzzati, P. A. Spegt, *Nature* **1967**, *215*, 701–704.
[10] A. N. Semenov, *Mol. Cryst. Liq. Cryst.* **1991**, *209*, 191–199; A. N. Semenov, S. V. Vasilenco, *Sov. Phys. JETP Engl. Transl.* **1986**, *63*, 70–79.
[11] D. R. M. Williams, G. H. Fredrickson, *Macromolecules* **1992**, *25*, 3561–3568.
[12] A. Halperin, *Macromolecules* **1990**, *23*, 2724–2731.
[13] E. Raphael, P. G. de Gennes, *Makromol. Chem. Macromol. Symp.* **1992**, *62*, 1–17.

Superconductivity and Chemical Bonding in Mercury

Shuiquan Deng, Arndt Simon,* and Jürgen Köhler

Dedicated to Professor Hartmut Bärnighausen on the occasion of his 65th birthday

Recently a hypothesis on the chemical origin of superconductivity was proposed which is based on a tendency for pairwise localization of conduction electrons.[1] In crystalline phases, in which chemical bonding is adequately described by the electronic band structure, a prerequisite for superconductivity seems to be the simultaneous occurrence of bands with large dispersion, "steep bands", and those with "flat bands" at the Fermi level E_F. The flat bands provide a vanishing Fermi velocity for some conduction electrons in the normal conducting state. This view is formally similar to a physical model based on the interplay of itinerant electrons in a wide band with local pairs of electrons in a narrow band.[2] However, in extracting the flat band/wide band features from calculated band structures we address the specific chemical bonding in actual superconductors.

Following arguments introduced by Krebs,[3] who suggested that the necessary condition for superconductivity is a crystal orbital that is nodeless in certain directions, Johnson and Messmer used SCF-Xα-SW cluster calculations to obtain remarkably accurate results for the superconducting characteristics of a number of elements and compounds.[4] However, this real space approach is based on clusters rather than infinite solids; in terms of a band structure, Γ point configurations are considered.

[*] Prof. Dr. A. Simon, Dr. S. Deng, Dr. J. Köhler
Max-Planck-Institut für Festkörperforschung
Heisenbergstrasse 1, D-70569 Stuttgart (Germany)
Fax: (+49) 711-689-1091
E-mail: remon@simpow.mpi-stuttgart.mpg.de

  1433-7851/98/3705-0640 $ 17.50+.50/0